

# Influence of confinement energy and band anticrossing effect on the electron effective mass in $\text{Ga}_{1-y}\text{In}_y\text{N}_x\text{As}_{1-x}$ quantum wells

Stanko Tomić\*

*Computational Science and Engineering Department, CCLRC Daresbury Laboratory, Warrington, Cheshire WA4 4AD, United Kingdom*

Eoin P. O'Reilly†

*Tyndall National Institute, Lee Maltings, Cork, Ireland*

(Received 1 November 2004; revised manuscript received 7 March 2005; published 9 June 2005)

We present a theoretical study of the electron effective mass in  $\text{Ga}_{1-y}\text{In}_y\text{N}_x\text{As}_{1-x}/\text{GaAs}$  quantum well (QW) structures. The calculations are based on a  $10 \times 10 \text{ k} \cdot \mathbf{p}$  band anticrossing Hamiltonian, incorporating valence, conduction, and nitrogen-induced bands. The results are tested by comparison with the experimentally determined electron effective mass in QWs with indium composition in the range between 10% and 50%, and nitrogen concentration between 1% and 5%. We report good agreement with experiment, confirming that the enhanced electron effective mass observed in the  $\text{Ga}_{1-y}\text{In}_y\text{N}_x\text{As}_{1-x}$  QW structures considered can be fully accounted for using the band anticrossing model.

DOI: 10.1103/PhysRevB.71.233301

PACS number(s): 73.21.Fg, 71.20.Nr

The quaternary semiconductor alloy  $\text{Ga}_{1-y}\text{In}_y\text{N}_x\text{As}_{1-x}$  has been attracting considerable interest. When a small amount of arsenic is replaced by nitrogen in  $\text{Ga}_{1-y}\text{In}_y\text{N}_x\text{As}_{1-x}$  the energy gap decreases rapidly, by  $\sim 0.1 \text{ eV}$  per percent of N for  $x < 3\%$ . This is of interest from a fundamental perspective and also because of its potential applications, opening the possibility of GaAs-based optoelectronic devices emitting in the  $1.3\text{--}1.5 \mu\text{m}$  telecommunications window. A major breakthrough in understanding this unusual behavior was achieved with the introduction of a two-level band anticrossing (BAC) model,<sup>1</sup> which describes the reduction in energy gap as due to a BAC interaction between the conduction band edge (CBE) and a band of nitrogen resonant defect states, which lie above the CBE in  $\text{Ga}_{1-y}\text{In}_y\text{N}_x\text{As}_{1-x}$ . The BAC model has successfully explained a wide range of experimental data, including the band-gap reduction in bulk  $\text{Ga}_{1-y}\text{In}_y\text{N}_x\text{As}_{1-x}$ ,<sup>2</sup> and the variation of the conduction band ground and excited state energies in  $\text{Ga}_{1-y}\text{In}_y\text{N}_x\text{As}_{1-x}$  quantum wells (QWs), as a function of N composition  $x$ , well width  $L$ , and applied hydrostatic pressure  $p$ .<sup>3-7</sup> It also explains a higher-lying feature (generally labeled  $E_+$ ) observed in photoreflectance measurements, and which occurs due to the mixing of conduction band edge character with the higher-lying N resonant states.<sup>8-10</sup>

The two-level BAC model has had limited success in describing the conduction band dispersion in bulk and QW structures. The model predicts an enhancement of the electron effective mass, due to the mixing that occurs between the conduction band and N resonant states. An enhanced effective mass has now been measured at the CBE in a wide range of  $\text{Ga}_{1-y}\text{In}_y\text{N}_x\text{As}_{1-x}$  samples. The observed enhancement in the in-plane electron effective mass is generally larger than expected in  $\text{GaN}_x\text{As}_{1-x}$  samples.<sup>11,12</sup> We have attributed this to the presence of defectlike states close to the CBE in  $\text{GaN}_x\text{As}_{1-x}$ ,<sup>13</sup> due to the random formation with increasing N composition  $x$  of N-N pairs, where two N atoms share a single Ga neighbor, and also the formation of larger clusters of N atoms. The N-N pairs introduce defect levels close to the GaAs CBE energy,<sup>14</sup> with larger clusters introducing states at even lower energy.<sup>15</sup> Detailed calculations

we have undertaken show that the CBE in  $\text{GaN}_x\text{As}_{1-x}$  can hybridize with N-related cluster states with which it is degenerate, or nearly degenerate. The hybridization leads to a marked reduction in the conduction band edge  $\Gamma$  character, fully consistent with the observed increase of the in-plane effective mass.<sup>13</sup>

The addition of indium to form  $\text{Ga}_{1-y}\text{In}_y\text{N}_x\text{As}_{1-x}$  has two main effects on the conduction band structure. First, the CBE shifts down in energy on an absolute scale with increasing  $y$  in  $\text{Ga}_{1-y}\text{In}_y\text{As}$ .<sup>16</sup> Second, because In has a larger atomic radius than Ga, there is a weaker overall lattice perturbation around an isolated N atom bonded to In neighbors, leading to a reduced BAC interaction. There is also a weaker distortion around N-N pairs and other cluster states, which when bonded predominantly to In neighbors consequently lie higher in energy compared to equivalent states in  $\text{GaN}_x\text{As}_{1-x}$ .<sup>17</sup> Improved agreement can be expected between the electron effective mass predicted by the BAC model and that observed experimentally when there are no cluster states close by in energy with which the  $\text{Ga}_{1-y}\text{In}_y\text{N}_x\text{As}_{1-x}$  CBE can interact. We show here that this is indeed the case for the  $\text{Ga}_{1-y}\text{In}_y\text{N}_x\text{As}_{1-x}$  samples which have been considered, confirming that, away from cluster states, the BAC model provides an excellent description not just of the energy gap but also of the band dispersion.

We first summarize below the BAC model. We then present the parameters that we use to describe the BAC interaction in  $\text{Ga}_{1-y}\text{In}_y\text{N}_x\text{As}_{1-x}$ . This is followed by a general analysis of the expected variation of effective mass with well width  $L$ , In composition  $y$ , and N composition  $x$  in  $\text{Ga}_{1-y}\text{In}_y\text{N}_x\text{As}_{1-x}/\text{GaAs}$  QW structures. Finally we compare our results with a range of experimental measurements on  $\text{Ga}_{1-y}\text{In}_y\text{N}_x\text{As}_{1-x}/\text{GaAs}$  QW structures, confirming that the measured electron effective mass in all  $\text{Ga}_{1-y}\text{In}_y\text{N}_x\text{As}_{1-x}$  samples reported to date is in excellent agreement with the value predicted using the BAC model.

It is well established that replacing a single As atom by N introduces a resonant defect level above the conduction band edge of GaAs.<sup>14,18</sup> The BAC model builds on this result, identifying the reduction in energy gap as due to an interac-

tion between the host matrix CBE, and a band of localized N resonant states above the CBE. The conduction band dispersion in bulk  $\text{Ga}_{1-y}\text{In}_y\text{N}_x\text{As}_{1-x}$  is then given in the BAC model by the lower eigenvalue  $E_-$  of the  $2 \times 2$  matrix

$$H(x) = \begin{pmatrix} E_N & V_{Nc} \\ V_{Nc} & E_c + \frac{\hbar^2 k^2}{2m_c^*} \end{pmatrix} \quad (1)$$

with the zone-center state at energy  $E_c$  associated with the extended CBE state  $\psi_{c0}$  of the  $\text{Ga}_{1-y}\text{In}_y\text{As}$  matrix,  $E_N$  the energy of the localized N resonant impurity state (with wave function  $\psi_N$ ), and  $V_{Nc}$  describing the interaction between the two bands. The band dispersion enters via the term involving  $m_c^*$ , the CBE relative effective mass of the host matrix given in units of the free electron mass ( $m_0$ ). As noted earlier, a resonant feature associated with the upper eigenvalue,  $E_+$ , has also been observed in photoreflectance measurements,<sup>8,9</sup> appearing in  $\text{GaN}_x\text{As}_{1-x}$  for  $x > \sim 0.2\%$ .

The band dispersion is calculated below by extending the conventional eight-band  $\mathbf{k} \cdot \mathbf{p}$  Hamiltonian to a ten-band model<sup>6,19</sup> to describe the band structure of  $\text{Ga}_{1-y}\text{In}_y\text{N}_x\text{As}_{1-x}$ , adding two (spin-degenerate) nitrogen-related bands from Eq. (1) to the usual two conduction and six valence band Bloch functions. The  $10 \times 10$   $\mathbf{k} \cdot \mathbf{p}$  model has been successfully used to describe the energy spectra and optical transitions in  $\text{Ga}_{1-y}\text{In}_y\text{N}_x\text{As}_{1-x}$  QWs,<sup>7</sup> and to describe the gain spectra as a function of carrier density in  $1.3 \mu\text{m}$  laser structures.<sup>19,20</sup> To set up the Hamiltonian matrix elements we used the same procedure as described in Ref. 19, with the material parameters for InAs and GaAs taken from Ref. 21, and the lattice constant, elastic constants, and deformation potentials of zinc-blende GaN and InN taken from Ref. 22.

Several studies support that the energy of the N resonant state and its coupling to the CBE vary with In composition in  $\text{Ga}_{1-y}\text{In}_y\text{N}_x\text{As}_{1-x}$ .<sup>4,23,24</sup> We assume the N resonant level to vary with In composition  $y$  as  $E_N$  (eV) =  $1.65 - 0.18y$ , where the zero of energy is taken at the GaAs valence band maximum. The host matrix unperturbed conduction band energy is assumed to vary with N composition  $x$  as  $E_c(y) - \alpha x$ , with  $\alpha$  (in eV) =  $1.55 - 0.14y$ , while the matrix element linking the N state and host matrix CBE is presumed to vary with N composition  $x$  and In composition  $y$  as<sup>23</sup>  $V_{Nc}$  (eV) =  $-(2.45 - 1.17y)\sqrt{x}$ . A similar trend in the coupling parameter  $V_{Nc}$  was found experimentally in a study where the nitrogen resonant level was kept fixed at 1.675 eV, independent of the indium composition in the different structures considered.<sup>24</sup>

We investigate the predicted influence of nitrogen and confinement energy on the electron in-plane effective mass by considering two sets of QW structures, for one of which we assume the N composition  $x = 1.1\%$ ,<sup>12,30</sup> while the other is assumed to be nitrogen-free ( $x = 0\%$ ). We assume the indium composition  $y = 25\%$  in both cases, and vary the QW width from  $L = 0.2$  to 15 nm.

Figure 1(a) shows the calculated variation at  $T = 4$  K of the in-plane band edge effective mass for the  $i$ th conduction subband,  $m_{ei}^*$ , as a function of QW width for  $x = 1.1\%$  (solid lines,  $i = 1, 2$ ), and for the nitrogen-free case (dashed lines,  $i = 1, 2, 3$ ). The effective masses were determined by numeri-

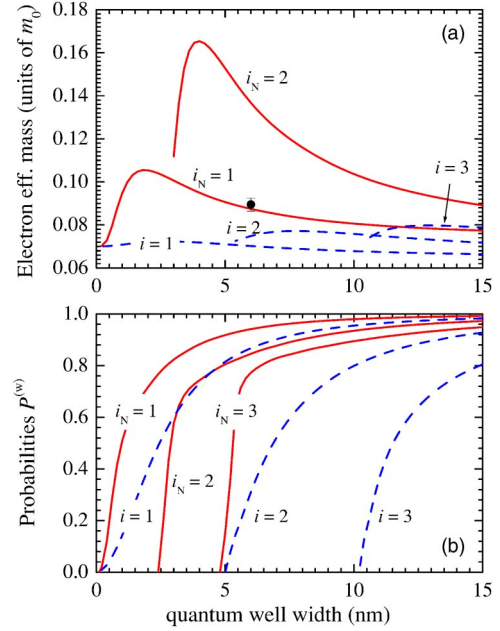


FIG. 1. (Color online) (a) In-plane electron effective mass of the first two confined subbands in  $\text{Ga}_{0.75}\text{In}_{0.25}\text{N}_{0.011}\text{As}_{0.989}$  QWs (solid line), and of the first three confined subbands in  $\text{Ga}_{0.75}\text{In}_{0.25}\text{As}$  QWs (dashed lines) as a function of the quantum well width  $L$ . Experimental point at  $L = 6$  nm,  $x = 1.1\%$ , and  $y = 25\%$  is taken from Ref. 12. (b) Probability  $P_i^{(w)}$  for an electron to be in the well region in  $\text{Ga}_{0.75}\text{In}_{0.25}\text{N}_{0.011}\text{As}_{0.989}$  QWs (solid line) and  $\text{Ga}_{0.75}\text{In}_{0.25}\text{As}$  QWs (dashed lines) as a function of the QW width.

cal differentiation of the calculated QW subband dispersion  $m_{e|i}^* = (\hbar^2 k_{||}) / |\partial E_{ei}(k_{||}) / \partial k_{||}|$ . In both cases, the in-plane effective mass approaches the bulk strained layer parallel mass in wide wells. Two significant differences can be observed in the N-containing wells. First, the calculated mass is enhanced for all well widths, due to the incorporation of nitrogen. Second, the calculated mass peaks quite sharply at intermediate well widths, just below  $L = 2$  nm for the lowest subband ( $i = 1$ ) and near  $L = 4$  nm for the first excited subband ( $i = 2$ ).

The increased mass at wide well widths follows directly from the BAC model of Eq. (1). The CBE effective mass in bulk  $\text{Ga}_{1-y}\text{In}_y\text{N}_x\text{As}_{1-x}$  [given by the variation of the lower eigenvalue  $E_-$  of Eq. (1) with  $k$ ] is larger than the host matrix effective mass  $m_c^*$  in Eq. (1). We can write

$$m_e^* = \frac{m_c^*}{|\alpha_c|^2}, \quad (2)$$

where  $m_e^*$  is the CBE effective mass of the  $\text{Ga}_{1-y}\text{In}_y\text{N}_x\text{As}_{1-x}$  alloy, and the wave function  $\psi_-$  of the  $E_-$  state is given in the two-level BAC model of Eq. (1) by

$$\psi_- = \alpha_c \psi_{c0} + \alpha_N \psi_N \quad (3)$$

where  $\alpha_{N(c)}$  denotes the amplitude of the  $E_-$  state projected onto the N resonant state (unperturbed CBE state) with  $|\alpha_N|^2 + |\alpha_c|^2 = 1$ .<sup>25</sup>

The mixing between the N level and the CBE of the host material therefore reduces the band dispersion in

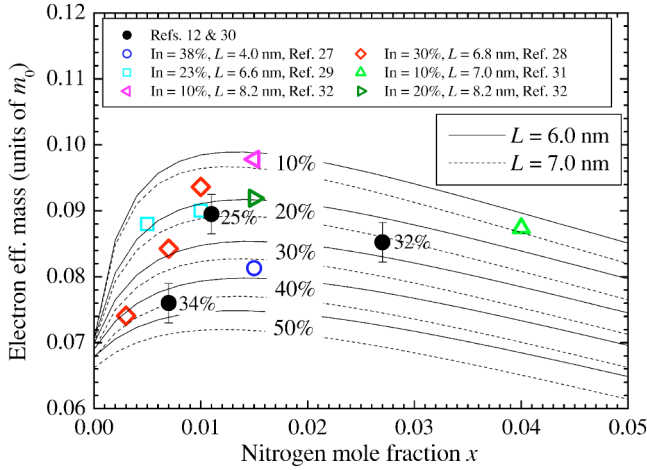


FIG. 2. (Color online) Calculated variation of the in-plane CBE electron effective mass as a function of N composition  $x$  in  $\text{Ga}_{1-y}\text{In}_y\text{N}_x\text{As}_{1-x}$  QWs for QW width  $L=6$  nm (solid lines) and  $L=7$  nm (dotted lines), and for  $y=10\%$  to  $50\%$  in  $10\%$  steps. Data points: experimental mass values taken from Refs. 12 (●), 29 (□), 28 (◇), 27 (○), 31 (△), and 32 (◁, ▷).

$\text{Ga}_{1-y}\text{In}_y\text{N}_x\text{As}_{1-x}$ . In addition, the dispersion of the lowest band is strongly nonparabolic, with the electron mass increasing rapidly with energy  $E$  and wave vector  $k$ . We therefore find that the calculated QW band edge mass tends to increase both as the confinement energy increases for a fixed well width, and also as the well width decreases for a given confined level until the QW confined state wave function starts to penetrate significantly into the barrier. The barrier wave function penetration then increases rapidly with further decrease of well width, causing the calculated effective mass value to drop off toward the barrier bulk mass value.

This is confirmed in Fig 1(b), which shows  $P_i^{(w)}$ , the probability of finding the  $i$ th electron confined state in the well region for the first three confined states ( $i=1, 2, 3$ ). (The probability of the  $i$ th state being in the barrier,  $P_i^{(b)}$ , is then given by  $P_i^{(b)}=1-P_i^{(w)}$ .) The solid lines are for the  $\text{Ga}_{0.75}\text{In}_{0.25}\text{N}_{0.011}\text{As}_{0.989}/\text{GaAs}$  QWs while the dashed lines show the variation for the nitrogen-free  $\text{Ga}_{0.75}\text{In}_{0.25}\text{As}/\text{GaAs}$  QWs. The addition of nitrogen reduces the wave function penetration into the barrier for a fixed well width. This arises because only the conduction band component  $\psi_{c0}$  of the wave function is continuous in Eq. (3) across the well/barrier interface;<sup>25,26</sup> the nitrogen-related component  $\psi_N$  drops abruptly to zero in the barrier. As the confinement energy increases, the magnitude of  $\alpha_c$  decreases; this tends both to reduce the wave function penetration into the barrier, and also to increase the average effective mass  $m_e^*$  within the well.

Having established the main factors that influence the electron effective mass in the BAC model, we now compare the calculated effective mass values with the experimentally determined values reported in the literature.<sup>12,27-32</sup> The majority of experimental measurements are for QWs of intermediate thickness (mainly  $L\sim 6-7$  nm), and with a wide range of In and N compositions,  $y$  and  $x$ . Figure 2 compares the calculated and experimentally measured ground state

( $i=1$ ) CBE electron effective mass  $m_e^*$  for a range of structures. In our calculations we choose the QW width as  $L=6$  (solid lines) and  $7$  nm (dotted lines) in order to compare with the experimentally determined trends in effective mass. We calculate the variation in in-plane effective mass when we change the indium concentration in the well from  $10\%$  to  $50\%$  in steps of  $10\%$ , while the nitrogen concentration is continuously varied from  $x=0$  to  $5\%$ .

Most of the experimental reports on  $\text{Ga}_{1-y}\text{In}_y\text{N}_x\text{As}_{1-x}$  are based on an indirect estimate of the electron effective mass via analysis of the interband transition energies.<sup>27-29,32</sup> This type of experiment probes the band dispersion and electron effective mass ( $m_{e\perp}^*$ ) along the growth direction, perpendicular to the quantum well plane. It was previously shown for a wide range of  $\text{GaN}_x\text{As}_{1-x}$  samples that the mass determined from such experiments is generally not influenced by the presence or otherwise of nitrogen cluster states.<sup>25</sup> We find that the same is true for the  $\text{Ga}_{1-y}\text{In}_y\text{N}_x\text{As}_{1-x}$  samples considered here.

For samples where the exciton mass is reported,<sup>12</sup> we extract an in-plane electron mass ( $m_{e\parallel}^*$ ) by first calculating the in-plane effective mass of the highest valence band in the  $\text{Ga}_{1-y}\text{In}_y\text{N}_x\text{As}_{1-x}/\text{GaAs}$  QWs considered, and then estimating the inverse electron mass based on the difference between inverse exciton and hole masses. For samples with  $(x,y,L)=(0.007,0.34,7$  nm),  $(0.011, 0.25, 6$  nm),  $(0.027, 0.32, 6$  nm), and  $(0.052, 0.38, 8.2$  nm), we estimate the heavy hole effective mass to be  $m_{\text{hh}\parallel}^*=0.11m_0$ ,  $m_{\text{hh}\parallel}^*=0.124m_0$ ,  $m_{\text{hh}\parallel}^*=0.11m_0$ , and  $m_{\text{hh}\parallel}^*=0.086m_0$ , respectively; these values are comparable to experimentally determined hole masses.<sup>33</sup> As shown in Fig. 2, the overall agreement between the experimental and theoretical results is very good for the whole range of concentrations considered. The calculations predict that the electron mass initially rises rapidly with N concentration, before reaching a peak value beyond which the mass then decreases slowly with increasing  $x$ . This trend is consistent with the general experimental data. The results of Pan *et al.*<sup>28</sup> show a wider scatter compared to the predicted values than is the case for the other results. This may reflect the indirect manner in which the mass values were deduced in this case, by fitting to interband transition energies rather than by a direct measurement which probes the conduction band dispersion in the QWs considered. It may also reflect any uncertainties in well width and composition. If we vary the well width in our calculations by  $\pm 0.5$  nm, the indium concentration by  $\pm 2\%$ , and allow the uncertainty in nitrogen composition to vary from  $\pm 30\%$  at low concentrations to  $\pm 10\%$  at  $x=0.05$ ,<sup>7</sup> we find a change in the calculated in-plane effective mass of  $\Delta m_{e\parallel}^* \approx \pm 0.004m_0$  for  $x \geq 0.005$ , dropping linearly to  $\sim 5.6 \times 10^{-4}$  for the nitrogen-free samples.

The generally good agreement found in all cases here between the BAC model and experiment is to be contrasted with the case of  $\text{GaN}_x\text{As}_{1-x}$ , where a consistent trend has been found of unexpectedly large in-plane mass values, such as  $m_{e\parallel}^*=0.13m_0$ ,  $0.12m_0$ , and even  $0.19m_0$  for  $x=0.1\%$ ,<sup>34</sup>  $1.2\%$ ,<sup>11</sup> and  $2.0\%$ .<sup>11</sup> All of these values lie well above the theoretical curves in Fig. 2. We have shown recently that the enhanced  $\text{GaN}_x\text{As}_{1-x}$  in-plane mass values are due to hybrid-

ization between the CBE and nitrogen cluster states close to the band edge. We conclude that adding indium shifts the CBE downward with respect to the cluster states, restoring the applicability of the BAC model for the samples whose in-plane mass is considered in Fig. 2.<sup>12</sup> We predict that the influence of higher-lying cluster states on the CBE could still be observed in  $\text{Ga}_{1-y}\text{In}_y\text{N}_x\text{As}_{1-x}$ , either by going to narrow QWs with larger confinement energy, or else through the application of hydrostatic pressure. The application of pressure shifts the CBE upward in energy relative to the N levels,<sup>1,14,18</sup> which should lead to a significant increase in  $m_{\text{ell}}^*$  as the CBE passes through the lowest N-related levels.

In summary, we have used a  $10 \times 10 \mathbf{k} \cdot \mathbf{p}$  band anticrossing Hamiltonian<sup>19</sup> to investigate the predicted variation of the conduction band edge effective mass with In and N com-

position, and with well width  $L$  in  $\text{Ga}_{1-y}\text{In}_y\text{N}_x\text{As}_{1-x}/\text{GaAs}$  QW structures. The predictions of our theoretical model agree very well with the experimentally determined results on both perpendicular and in-plane electron effective masses for the same range of material composition and QW widths. Our results confirm the validity of the ideas underpinning the BAC model, showing that it can be used for the reliable prediction of the electron effective masses in a wide range of  $\text{Ga}_{1-y}\text{In}_y\text{N}_x\text{As}_{1-x}$  quantum wells and optoelectronic devices based on this material system.

The authors are grateful to the Engineering and Physical Sciences Research Council (U.K.) and Science Foundation Ireland for supporting this work. We thank A. Lindsay and A. Polimeni for useful discussions.

\*Email address: s.tomic@dl.ac.uk

†Email address: eoreilly@tyndall.ie

<sup>1</sup>W. Shan, W. Walukiewicz, J. W. Ager III, E. E. Haller, J. F. Geisz, D. J. Friedman, J. M. Olson, and S. R. Kurtz, *Phys. Rev. Lett.* **82**, 1221 (1999).

<sup>2</sup>A. Lindsay and E. P. O'Reilly, *Solid State Commun.* **112**, 443 (1999).

<sup>3</sup>H. Grüning, L. Chen, Th. Hartmann, P. J. Klar, W. Heimbrod, F. Höhnsdorf, J. Koch, and W. Stolz, *Phys. Status Solidi B* **215**, 39 (1999).

<sup>4</sup>P. J. Klar, H. Grüning, J. Koch, S. Schäfer, K. Volz, W. Stolz, W. Heimbrod, A. M. Kamal-Saadi, A. Lindsay, and E. P. O'Reilly, *Phys. Rev. B* **64**, 121203(R) (2001).

<sup>5</sup>C. Skierbiszewski, P. Perlin, P. Wisniewski, T. Suski, J. F. Geisz, K. Hingerl, W. Jantsch, D. E. Mars, and W. Walukiewicz, *Phys. Rev. B* **65**, 035207 (2001).

<sup>6</sup>E. P. O'Reilly, A. Lindsay, S. Tomić, and M. Kamal-Saadi, *Semicond. Sci. Technol.* **17**, 870 (2002).

<sup>7</sup>S. A. Choulis, T. J. C. Hosea, S. Tomić, M. Kamal-Saadi, A. R. Adams, E. P. O'Reilly, B. A. Weinstein, and P. J. Klar, *Phys. Rev. B* **66**, 165321 (2002).

<sup>8</sup>J. D. Perkins, A. Mascarenhas, Y. Zhang, J. F. Geisz, D. J. Friedman, J. M. Olson, and S. R. Kurtz, *Phys. Rev. Lett.* **82**, 3312 (1999).

<sup>9</sup>P. J. Klar, H. Grüning, W. Heimbrod, J. Koch, F. Höhnsdorf, W. Stolz, P. M. A. Vicente, and J. Camassel, *Appl. Phys. Lett.* **76**, 3439 (2000).

<sup>10</sup>A. Lindsay and E. P. O'Reilly, *Physica E (Amsterdam)* **21**, 901 (2004).

<sup>11</sup>P. N. Hai, W. M. Chen, I. A. Buyanova, H. P. Xin, and C. W. Tu, *Appl. Phys. Lett.* **77**, 1843 (2000).

<sup>12</sup>G. Baldassarri Höger von Högersthal, A. Polimeni, F. Masia, M. Bissiri, M. Capizzi, D. Gollub, M. Fischer, and A. Forchel, *Phys. Rev. B* **67**, 233304 (2003).

<sup>13</sup>A. Lindsay and E. P. O'Reilly, *Phys. Rev. Lett.* **93**, 196402 (2004).

<sup>14</sup>X. Liu, M.-E. Pistol, L. Samuelson, S. Schwetlick, and W. Seifert, *Appl. Phys. Lett.* **56**, 1451 (1990).

<sup>15</sup>P. R. C. Kent, L. Bellaiche, and A. Zunger, *Semicond. Sci. Technol.* **17**, 851 (2002).

<sup>16</sup>C. G. Van de Walle, *Phys. Rev. B* **39**, 1871 (1989).

<sup>17</sup>A. Lindsay (unpublished).

<sup>18</sup>D. J. Wolford, J. A. Bradley, K. Fry, and J. Thompson, in *Proceedings of the 17th Conference on the Physics of Semiconductors* (Springer, New York, 1984), p. 627.

<sup>19</sup>S. Tomić, E. P. O'Reilly, R. Fehse, S. J. Sweeney, A. R. Adams, A. D. Andreev, S. A. Choulis, T. J. C. Hosea, and H. Riechert, *IEEE J. Sel. Top. Quantum Electron.* **9**, 1228 (2003).

<sup>20</sup>M. Hofmann, A. Wagner, C. Ellmers, C. Schlichenmeier, S. Schaffer, F. Höhnsdorf, J. Koch, W. Stolz, S. W. Koch, W. W. Ruhle, J. Hader, J. V. Moloney, E. P. O'Reilly, B. Borchert, A. Y. Egorov, and H. Riechert, *Appl. Phys. Lett.* **78**, 3009 (2001).

<sup>21</sup>I. Vurgaftman, J. R. Meyer, and L. R. Ram-Mohan, *J. Appl. Phys.* **89**, 5815 (2001).

<sup>22</sup>I. Vurgaftman and J. R. Meyer, *J. Appl. Phys.* **94**, 3675 (2003).

<sup>23</sup>A. Lindsay and E. P. O'Reilly, *Physica B* **340–342**, 434 (2003).

<sup>24</sup>M. Hetterich, A. Grau, A. Yu. Egorov, and H. Riechert, *J. Appl. Phys.* **94**, 1810 (2003).

<sup>25</sup>S. Tomić, E. P. O'Reilly, P. J. Klar, H. Grüning, W. Heimbrod, W. M. Chen, and I. A. Buyanova, *Phys. Rev. B* **69**, 245305 (2004).

<sup>26</sup>M. Hetterich, A. Grau, A. Yu. Egorov, and H. Riechert, *J. Phys.: Condens. Matter* **16**, S3151 (2004).

<sup>27</sup>M. Hetterich, M. D. Dawson, A. Yu. Egorov, D. Bernklau, and H. Riechert, *Appl. Phys. Lett.* **76**, 1030 (2000).

<sup>28</sup>Z. Pan, L. H. Li, Y. W. Lin, B. Q. Sun, D. S. Jiang, and W. K. Ge, *Appl. Phys. Lett.* **78**, 2217 (2001).

<sup>29</sup>J.-Y. Duboz, J. A. Gupta, M. Byloss, G. C. Aers, H. C. Liu, and Z. R. Wasilewski, *Appl. Phys. Lett.* **81**, 1836 (2002).

<sup>30</sup>A. Polimeni, M. Bissiri, G. Baldassarri Höger von Högersthal, M. Capizzi, D. Giubertoni, M. Barozzi, M. Bersani, D. Gollub, M. Fischer, and A. Forchel, *Solid-State Electron.* **47**, 447 (2003).

<sup>31</sup>M. H. Gass, A. J. Papworth, T. B. Joyce, T. J. Bullough, and P. R. Chalker, *Appl. Phys. Lett.* **84**, 1453 (2004).

<sup>32</sup>J. B. Héroux, X. Yang, and W. I. Wang, *J. Appl. Phys.* **92**, 4361 (2002).

<sup>33</sup>A. Polimeni, F. Masia, A. Vinattieri, G. Baldassarri Höger von Högersthal, and M. Capizzi, *Appl. Phys. Lett.* **84**, 2295 (2004).

<sup>34</sup>F. Masia, A. Polimeni, G. Baldassarri Höger von Högersthal, M. Bissiri, M. Capizzi, P. J. Klar, and W. Stolz, *Appl. Phys. Lett.* **82**, 4474 (2003).